LUNDS UNIVERSITET

Growth of PdO on Pd(100)

Isac Bramer

Bachelor of Science

Project Duration: 3 months

Supervisors: Johan Gustafson and Hanna Sjö

Division of Synchrotron Radiation Research

14th May 2024

This thesis is submitted for the degree of
Bachelor of Theoretical Physics
at the Department of Physics,
Lund University.

Abstract

This thesis explores the growth of palladium oxide (PdO) on palladium(100) surfaces, focusing particularly on how different environmental conditions affect the formation and stability of various PdO orientations rellative to the Pd substrate. The motivation of the project is that catalytic oxidation of methane, is believed to be strongly dependent on the surface structure of the involved catalyst. Gaps remain in understanding how specific PdO surface planes form and stabilize under different conditions and how these planes influence catalytic activity for methane oxidation.

The aim of this study was to understand the formation processes of PdO surface planes such as PdO(100) and PdO(101) under varying temperatures and oxygen pressures. Using grazing incidence X-ray diffraction (GIXRD), this research systematically analyzed how these surfaces respond to changes in environmental conditions, with a hypothesis that different temperatures and oxygen pressures promote the formation of a variety of PdO planes.

The methodology involved detailed GIXRD experiments conducted at temperatures ranging from 250°C to 400°C, with oxygen pressures from 2×10^{-4} mbar to 100 mbar. This approach allowed for observations of the formation of PdO planes on the Pd(100) substrate, providing data on their structural configurations.

Findings reveal that higher temperatures and pressures indeed facilitate the formation of diverse PdO planes. Higher temperature also appears to facilitate the formation of multiple different planes on the same surface. At low temperatures we found the PdO(201) orientation, a result not previously documented in previous literature.

This study contributes to the field of catalysis by attempting to detail the conditions under which different PdO planes form and by highlighting the potential catalytic differences of these planes. The hope is with these gained insights along with future research to develop more effective catalysts particularly for methane oxidation.

Contents

Abbreviations

The following abbreviations are used throughout this thesis to denote various scientific terms.

GIXRD Grazing Incidence X-ray Diffraction: A technique used to analyze the surface structures of crystalline materials.

SXRD Surface X-ray Diffraction: A technique used to analyze the surface structures of crystalline materials.

XRD X-ray Diffraction: A technique for determining the atomic and molecular structure of a crystal.

FCC Face-Centered Cubic: A type of crystal structure.

BCC Body-Centered Cubic: A type of crystal structure.

1 Introduction

Catalysis is essential in the chemical industry for speeding up reactions, making processes more efficient, and can turn harmful pollutants into less damaging substances. One significant example is the transformation of methane a major greenhouse gas—into less potent substances like carbon dioxide through catalytic oxidation.

Optimizing the process using catalysts like palladium oxide (PdO) remains challenging since much is still unknown. The catalyst efficiency has been shown to depend on surface structure, which will vary depending on the condition during growth[20]. Some of the condition dependent behavior has been studied.

Here we will focus on how different PdO surface orientations form and stabilize under varying temperatures and oxygen pressures. This research aims to explore this by employing X-ray diffraction to analyze how these surfaces respond to changes in environmental conditions. The hypothesis was that by manipulating temperature and oxygen pressure, the PdO (100) and (101) planes would form on the Pd(100) surface of which the (101) plane is believed to be the better catalyst especially for methane oxidation. The findings from this study confirm that, the orientation of the PdO depend on the temperature and oxygen pressure, and that some of the planes, such as PdO(201), are more stable than expected and potentially more important in catalysis than previously recognized.

These results may be significant as they contribute to a better understanding of PdO, offering insights that could lead to more efficient methane oxidation processes. Knowing which PdO surfaces form under specific conditions is a crucial step before continued research can follow.

2 Theory

2.1 Crystal Structure

The study of crystal structures is essential for the properties of materials. A crystal structure is defined by its lattice. This lattice represents the symmetry and spatial organization of the crystal and is fundamental in defining the crystal's physical properties. Attached to each point of this lattice is a basis, a group of one or more atoms that are repeated throughout the crystal in a consistent pattern, forming the actual substance of the crystal. In crystallography, the unit cell is a volume that encapsulates the crystal's entire lattice pattern and, when tessellated in space, recreates the entire crystal. For materials such as palladium (Pd) and its oxide (PdO), the unit cells reflect unique lattice parameters: edge lengths ($\mathbf{a}_1$, $\mathbf{a}_2$, $\mathbf{a}_3$) and the angles between these edges. Pd, with its face-centered cubic (FCC) structure, has unit cells with equal edge lengths and 90-degree angles, signifying high symmetry and close packing. PdO crystallizes in a tetragonal structure, reflecting a different set of symmetries and lattice parameters.[7] In the context of real-space lattices, any point in the lattice can be described by the vector $\mathbf{R}$, defined as:

$$\mathbf{R} = m_1\mathbf{a_1} + m_2\mathbf{a_2} + m_3\mathbf{a_3}$$

where m_1, m_2, and m_3 are integers, and $\mathbf{a_1}, \mathbf{a_2}, \mathbf{a_3}$ are the lattice vectors. This equation explains the periodicity and structure of the crystal.

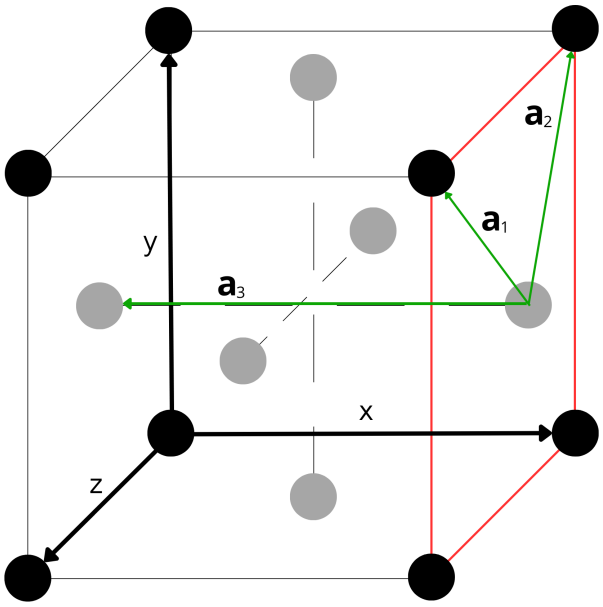

Figure 1: The FCC Pd unit cell showing a Pd atom in each corner of the cube in black as well as an atom in the centre of each side in grey. The side marked in red lines show the (100) plane which was used in this study. The $\mathbf{a}_1$, $\mathbf{a}_2$ and $\mathbf{a}_3$ vectors in green show the real-space unit vectors for the Pd(100) crystal.

Surface Lattices: The surface lattice of a crystal is a two-dimensional representation of the three-dimensional structure as projected onto a particular plane, designated by Miller indices. These indices (hkl) denote the orientation of the surface relative to the crystal's unit cell. In the case of Pd(100) or PdO(100), the (100) surface lattice is oriented parallel to the y-z plane of the unit cell, representing an atomic arrangement that is visible when viewing the crystal from the side, perpendicular to the x-axis.

The Pd(100) crystal lattice can be described as a tetragonal unit cell with two vectors in the surface plane $\mathbf{a}_1 = \mathbf{a}_2 = \sqrt{3.89}$ Å $= 2.75$ Å and one perpendicular to the surface plane $\mathbf{a}_3 = 3.89$ Å

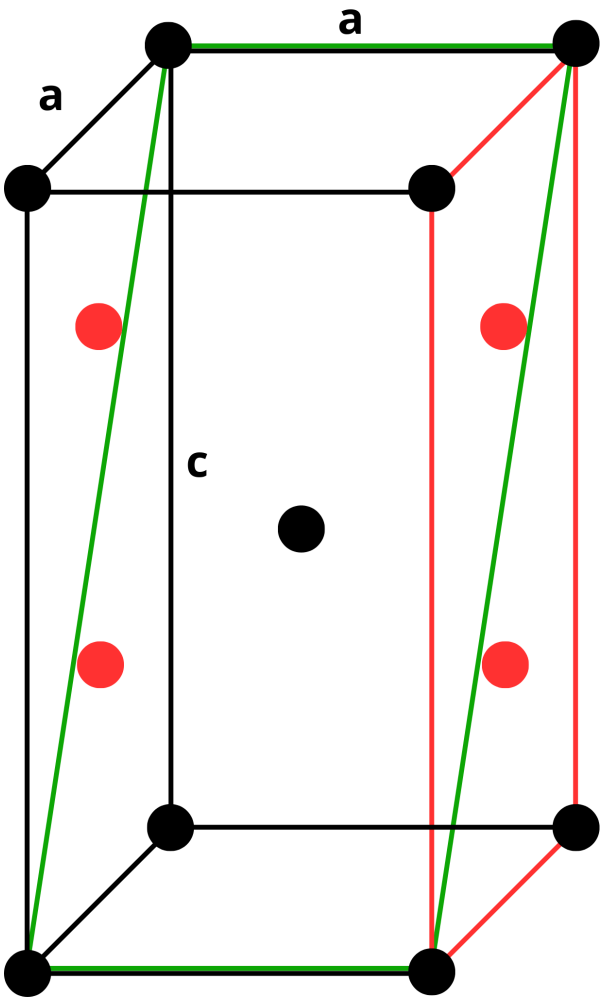

Figure 2: PdO unit cell showing all Pd atoms in black at each corner and in the centre. The oxygen (O) atoms are depicted in red. The side marked in red lines show the (100) plane and the plane in green shows the (101) plane. Here a = 3.04 Å and c = 5.328 Å showing the length of the black lines.

Different surface orientations exposes unique arrangements of Pd and O atoms. The (101) and (201) orientations depicted in the figures 2 and 3 both cut across the tetragonal unit cell. The orientation of these surface atoms have a great impact on the reactivity of PdO.

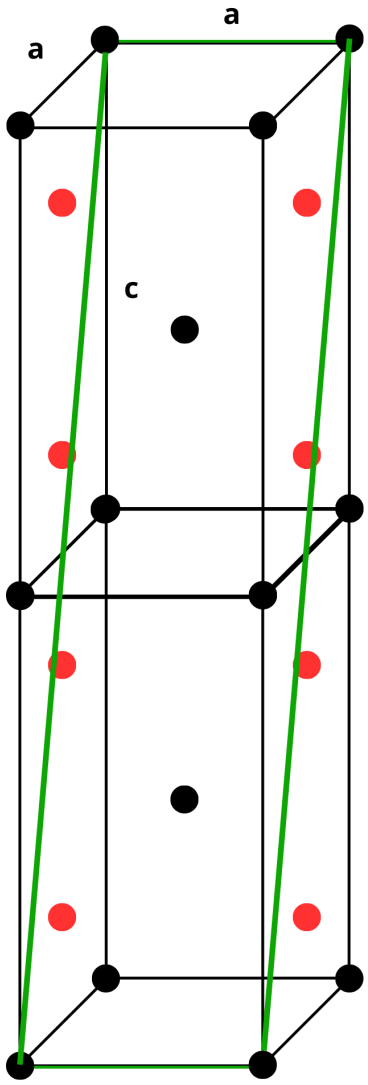

Figure 3: PdO unit cells showing all Pd atoms in black and oxygen atoms in red. The plane in green shows the (201) plane. Here a = 3.04 Å and c = 5.328 Å showing the length of the black lines.

2.2 Oxidation

Oxidation on palladium surfaces, particularly on Pd(100), creates the formation of a bulk oxide layer, PdO. This process changes both the chemical composition and the geometric arrangement of the atoms at the crystal surface, which can be depicted in section 3.1.

The focus of this work is on how these bulk oxide layers form and stabilize under various conditions. For Pd(100), the interaction between oxygen atoms and the palladium surface leads to a well-defined oxide layer. The formation of PdO on Pd(100) involves a series of steps where oxygen atoms adsorb on the surface, diffuse, and react with palladium atoms to form the oxide.[12]

Previous studies have shown that the crystallographic orientation of palladium, such as the (100) surface, influences the oxidation process. The Pd(100) surface tends to form the (100) and (101) PdO planes,[20] however the (201) plane has been frequently observed in this study as well.

The kinetics of oxide layer formation on Pd(100) and its subsequent stability have been studied, revealing that temperature and oxygen pressure, affect the growth rate and characteristics of the PdO layer.[11] The initial oxide formation has also been shown to affect the subsequent oxide growth of the surface structure.

2.3 X-Ray Diffraction

X-ray diffraction is a method in crystallography for determining the atomic-scale structure within crystalline materials. This process can be described by either Bragg's Law or the Laue condition, which both describe the interaction of X-rays with crystal lattices in the framework of vector formalism.

The reciprocal lattice is the Fourier transform of the real-space lattice, and is needed to understand diffraction. The reciprocal lattice vector $\mathbf{G}$, is defined as:

$$\mathbf{G} = \mathbf{q}_1\mathbf{b_1} + \mathbf{q}_2\mathbf{b_2} + \mathbf{q}_3\mathbf{b_3}$$

where q_i are integers, and the $\mathbf{b_i}$ are the basis vectors of the reciprocal lattice, described in more detail in section 3.5. They are constructed to be orthogonal to the real-space lattice vectors $\mathbf{a_i}$ such that $\mathbf{a_i} \cdot \mathbf{b_j} = \delta_{ij}2\pi$, with δ_{ij} being the Kronecker delta.

The Laue condition complements this by addressing the conditions for diffraction through the vector change $\Delta\mathbf{k}$, the difference between the incident ($\mathbf{k}$) and diffracted ($\mathbf{k}'$) wave vectors:

$$\Delta\mathbf{k} = \mathbf{k}' - \mathbf{k} = \mathbf{G}$$

This expression establishes that diffraction occurs when $\Delta\mathbf{k}$ is equivalent to a reciprocal lattice vector, leading to the phase alignment of scattered waves and hence, to constructive interference.[3]

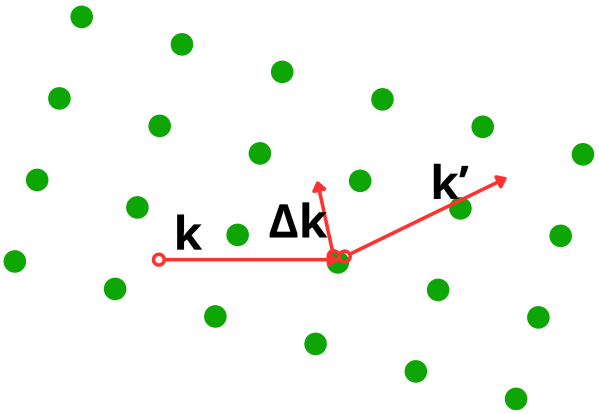

Figure 4: Figure representing the k, k' and Δk vectors.

To further explain the Laue condition, consider the scattering vector $\mathbf{Q}$, defined as:

$$\mathbf{Q} = \mathbf{k}' - \mathbf{k}$$

Constructive interference across the crystal lattice is observed when $\mathbf{Q}$ equals $\mathbf{G}$, aligning with the reciprocal lattice. For such interference to be observed throughout the entire lattice, for any lattice vector $\mathbf{R}$, the condition

$$e^{i\mathbf{Q}\cdot\mathbf{R}} = 1$$

must be satisfied, which simplifies to:

$$\mathbf{Q} \cdot \mathbf{R} = 2\pi n$$

where n is an integer. This relationship indicates that $\mathbf{Q}$, when expressed as a sum of the reciprocal lattice basis vectors scaled by integers h, k, and l, must equal a reciprocal lattice vector for constructive interference to occur.[3]

2.4 Reciprocal Lattice

The intensity of the diffracted waves at different spots is determined by the structure factor F, which reflects the specific atomic arrangement within the unit cell. This factor varies from one diffracted beam to another, influencing the intensity based on the atomic positioning within the crystal structure. The structure factor is given by:

$$F_{hkl} = \sum_j f_j e^{-2\pi i(hx_j + ky_j + lz_j)}$$

where f_j is the atomic form factor of the j-th atom, hkl are the Miller indices of the reflecting plane, and x_j, y_j, z_j represent the fractional coordinates of each atom within the unit cell. This restriction results from the symmetrical arrangement of atoms, which

also affects the phase of the scattered waves, ensuring that constructive interference and thus observable diffraction peaks occur under these conditions.
The FCC lattice such as the Pd crystal is characterized by atoms at each of the face centers, in addition to those at the corners, this is shown in figure 1. For FCC crystals, the above condition and hence diffraction peaks occur when the indices $h + k + l$ are either all even or all odd.

The differences in these diffraction conditions between lattices lead to distinct X-ray diffraction patterns, which can be utilized to identify and characterize materials based on their internal crystal structures. These patterns allows for precise determination of material properties and aids in the identification of crystallographic defects that might affect material performance[6]

2.5 Deriving Reciprocal Vectors

The real-space basis vectors together form the unit cell of a crystal. These vectors $\mathbf{a}_1$, $\mathbf{a}_2$ and $\mathbf{a}_3$ are constructed to be orthogonal to the reciprocal-space lattice vectors $\mathbf{b}_1$, $\mathbf{b}_2$ and $\mathbf{b}_3$ such that $\mathbf{a_i} \cdot \mathbf{b_j} = \delta_{ij} 2\pi$, with δ_{ij} being the Kronecker delta.[6] The theoretical value of each relevant vector for this study can be found in the table below.

Table 1: Value of each real-space and reciprocal-space vector for the different planes

	$\mathbf{a}_1$(Å)	$\mathbf{a}_2$(Å)	$\mathbf{a}_3$(Å)	$\mathbf{b}_1$(Å^{-1})	$\mathbf{b}_2$(Å^{-1})	$\mathbf{b}_3$(Å^{-1})
Pd(100)	2.75	2.75	3.89	2.28	2.28	1.62
PdO(100)	3.04	5.33	3.04	2.07	1.78	2.07
PdO(101)	3.04	4.32	10.56	2.07	1.45	0.59
PdO(105)	3.04	16.11	28.56	2.07	0.39	0.22

3 Methodology

3.1 Setup

The diffraction experiments were conducted using a setup comprising an X-ray source, a sample in a vacuum chamber, and a detector. The X-ray source generated a beam directed towards the sample, which was placed in the chamber. The chamber had of three valves which made it possible to flow either oxygen or argon. The chamber was pumped using a turbo pump to keep the desired pressure. The chamber was a beryllium cylinder which has low adsorption coefficient to minimize the loss of intensity. A large 2D detector (Pilatus 300K) was placed opposite to the X-ray source. The vacuum chamber maintained ultra-high vacuum conditions around 10^{-8} mbar when no Oxygen (O_2) or Argon (Ar) was allowed in to prevent any atmospheric interference during or in between measurements.

3.2 Sample Preparations

Positioned inside a vacuum chamber, the crystal was sputtered with Ar ions at a pressure of 2×10^{-4} mbar and a current of 10 mA for 20 minutes. Following this, the sample was annealed at approximately 800°C, for 5 minutes. The annealing-sputtering cycle was repeated three times. This cleaning cycle ensured the surface was clean and reoriented into a flat Pd(100) structure.

3.3 Oxidizing the Sample

The sample was oxidized at different oxygen pressures and temperatures (see Table 1).

Table 2: Oxidation conditions for the Pd(100) sample across different rounds.

Oxidation Round	**Oxygen Pressure (mbar)**	**Temperature (°C)**
First Round	1	250, 300, 350, 400
Second Round	(2×10^{-4}), 1	300 (pre-oxidation), 250, 300, 350, 400
Third Round	100	250, 300, 350, 400

All oxidation rounds were done under 15 min of heating apart from the pre-oxidation phase in the second round which also involved an oxidation at 300°C for 5 minutes
Temperature adjustments were managed by altering the current to the heating element beneath the sample, with prior calibration linking current input to temperature. The temperatures used were 250°C, 300°C, 350°C, and 400°C.

3.4 Measurements

Diffraction measurements were performed by directing X-rays with a wavelength of 0.71 nm at the crystal, which was set at a grazing angle $\mu = 0.2^{\circ}$ relative to the beam. The

resulting diffraction patterns were recorded by the detector across a range of angles rotating the sample. For comprehensive coverage, the sample was rotated 180°, facilitating the generation of 360 scans at 0.5° intervals, each with an exposure time of one minute. The tetragonal symmetry of the crystal meant that a full 360° rotation was unnecessary, as each reflection would recur every 90°. This methodology was consistent across all measurement rounds.

In each scan, the image angle at which the PdO diffraction peaks occurred were found. The coordinates of the PdO peaks were then noted and later used to find what plane and Bragg reflection was observed. The scans done at the same temperature from the different rounds of measurements were added together and the sum of all the intensities were taken creating the pictures seen in the results section.

4 Analysis

Analyzing the measurements involves interpreting the observed surface planes on the crystal. This process starts by considering the position of the pixel where each reflection is observed relative to the location of the source. Since we know the distances from the source to the detector and the distance between each pixel as well as the distance between the reflection and the source we can calculate the **k** vector. With the wavelength of the X-ray, we can determine the **k'** vector and hence calculate the **Q** vector.

To identify which surface structure plane and reflection the measured **Q** vector correspond to, the measured **Q** was plotted along with theoretical **Q** vectors. The expected structures for the oxide structures described in section 3.5 was used to identify the Bragg reflections and planes. The vectors were plotted one plane at a time starting with the PdO(100) plane. The theoretical vectors were then rotated around the measured vector as seen in the figure 5 below. To find the closes match the magnitude was compared and the structure checked to see if it was an allowed peak. Measured reflections not corresponding to any allowed theoretical peak indicates that reflection is ordered in a different surface plane. Identifying which plane the remaining peaks correspond to was done by rotating the PdO(100) plane by an angle equal to the angle of an unmatched reflection. This rotation angle was used to identify a surface plane with the same angle. The unit cell and the corresponding real and reciprocal vectors described in section 3.5 were used to plot the new theoretical vectors for the identified surface plane.

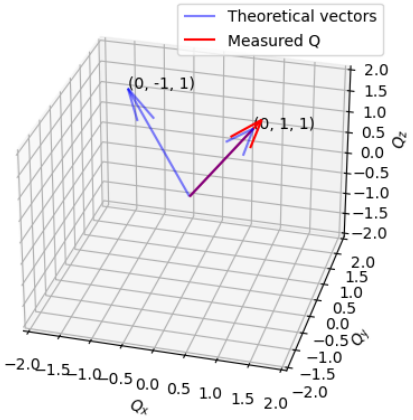

Figure 5: Plot of measured **Q** vector in red together with the theoretical vectors for PdO(100) in blue. Only the theoretical vectors with a similar angle to the measured one as shown. The blue vectors were rotated to clearly compare the different vectors. Here the measured value came from the PdO(100)_011 reflection. Units for the vectors are $Å^{-1}$

5 Results

After oxidising Pd(100) under various environmental conditions. The detector images from the XRD measurements show a range of different orientations of PdO in the near-surface region as well as under which conditions they form.

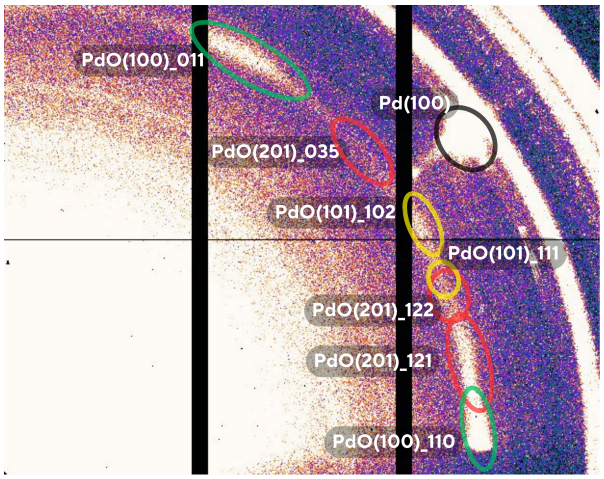

Figure 6: Sum of all scans: Markings in red are for the PdO(201) plane, in black is for the Pd(100) bulk, yellow are for the PdO(101) plane and green is for the PdO(100) plane. The numbers after the underscore show which Bragg reflection we observe. The rings further out are from the beryllium chamber.

In figure 6 three different orientations of PdO were observed, namely with (100), (101) and the (201) planes parallel to the surface. The reflections from the (100) plane had relatively high intensity and appeared very clearly. Additionally the PdO(201)_121 peak appeared frequently with high intensity as well. The PdO(201)_035 peak may appear almost non existent however this is since all measurements are added together, for some measurements mainly under 300°C the peak is seen more clearly also shown later in figure 7.

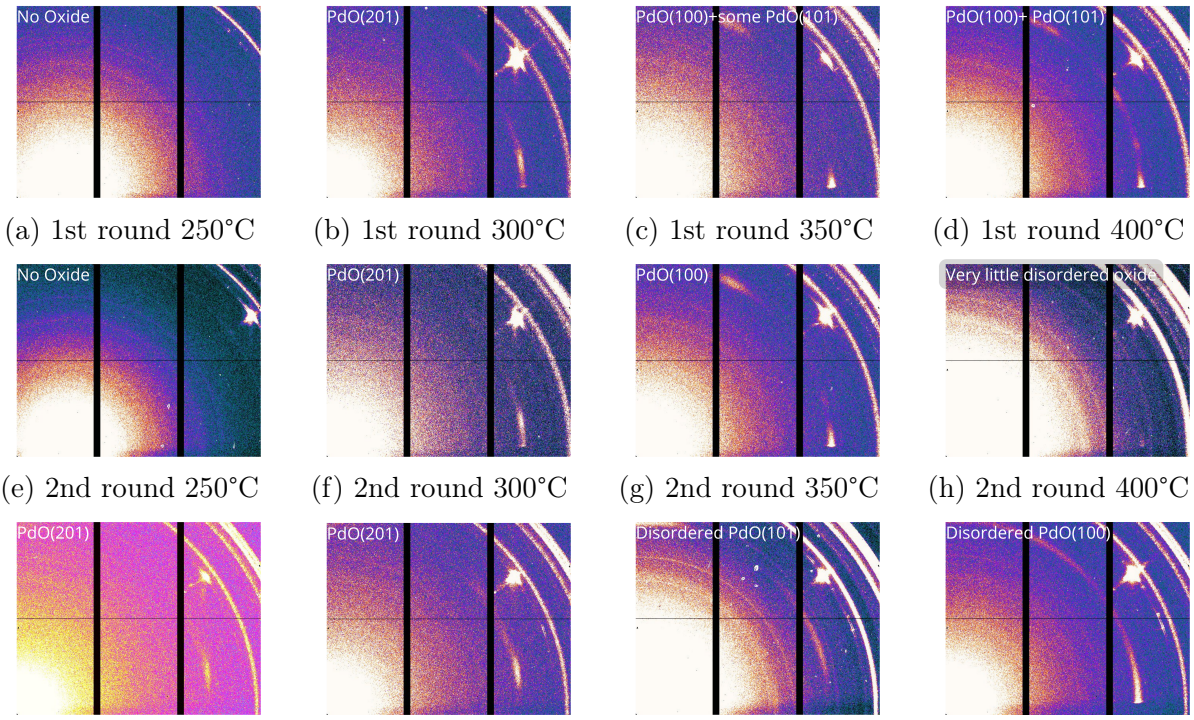

(a) 1st round 250°C (b) 1st round 300°C (c) 1st round 350°C (d) 1st round 400°C

(e) 2nd round 250°C (f) 2nd round 300°C (g) 2nd round 350°C (h) 2nd round 400°C

(i) 3rd round 250°C (j) 3rd round 300°C (k) 3rd round 350°C (l) 3rd round 400°C

Figure 7: The sum of all detector images for each individual measurement. The oxidation rounds are divided by rows and the temperature differences are divided by columns.

From figure 7 we see the result of all detector images added together separately for each measurement. Observing the peaks highlighted in figure 5 it shows that different conditions provide different oxide growth. From the pictures a and e on the left side done a 250°C no oxide growth was observed. However in picture i done at the higher pressure of 100 mbar we do see the PdO(201)_121 reflection.

The measurements done at 300°C show very slight differences where the main difference is that the second round measurement show the PdO(201)_035 oxide much fainter.

For the lower pressure measurements done at 350°C the (100) plane is very dominant and only the (201) plane is observed in the second round. The first round does appear to have some faint (101) orientation as well. However with higher pressure the (101) plane dominates instead with some possible (201) formation as well.

There are large differences in the different measurements done at 400°C. The first round formed very clear and distinct peaks for the (100) and (101) orientations. The second round showed almost no oxide formation. Only some very faint PdO(101)_102 reflections could be observed. The third round with the high pressure showed a strongly disordered orientations where with (100) the most prevalent.

6 Discussion

Research on crystal formation under conditions ranging from pressures between $10^{-}4$ mbar and 1 bar as well as temperatures between 200°C and 800°C, indicates that the formation of specific crystal planes, such as the one with the lowest energy state in oxides like PdO, can be influenced significantly by environmental factors [14]. These studies suggest that at lower energy or pressure levels, certain crystal planes, which are energetically more favorable, are more likely to form due to the direct relationship between the formation energy of a crystal plane and its stability under given conditions.

During the initial two rounds of measurements conducted at 1 mbar O_2 and 250°C, no surface oxides were detected. This suggests that under these conditions, neither the energy available nor the O_2 pressure was sufficient to facilitate oxide formation. This aligns with previous findings, which indicated that lower oxygen pressures and temperatures often fail to achieve the oxidative environment necessary for PdO formation [16]. Upon increasing the O_2 pressure to 100 mbar, the formation of thin bulk-oxides with the PdO(201) orientation was observed, corroborating the theory that higher oxygen pressures can overcome the kinetic barriers to oxide formation, as discussed in studies on Gibbs free energy of PdO [17]. This observation underlines the critical role of environmental conditions in determining the phase stability and structure of surface oxides. The observation of only one type of oxide plane, combined with the absence of oxides under lower pressures, implies that the oxides that did form are those that need the least additional energy to form. A possible explanation to why the (201) orientation forms could be that the movement needed of atoms to transition into PdO is relatively low. This is also show in the close match seen in figure 8. This formation then prohibits the (101) orientation to some extent as transforming one orientation to another is difficult although the (101) orientation is likely more stable.

Regarding oxidation under high pressure and temperature, materials may undergo phase transformations or adopt different crystal structures that minimise the system's free energy. This phenomenon is shown in a study that discusses how different polymorphs, or crystal forms, have the lowest energy under specific pressure-temperature conditions, suggesting that similar principles apply to oxide formation like PdO [15]. Under conditions where lower pressures and temperatures prevent the formation of oxides, increasing the pressure can shift the equilibrium, promoting the formation of more stable oxide planes. This is also reaffirmed in the fact that no oxides were observed before the pressure was increased under the 250°C measurements.

This would also explain why at temperatures suitable for oxide formations, some planes form under 1 mbar while not at 100 mbar although the temperature is the same. As depicted when the (100)plane formed after the 300°C oxidation for the first two sets of measurements while not for the 100 mbar O_2 measurement.

Further emphasizing the influence of crystal structure on oxide stability, previous re-

search has found the PdO(101) plane to be more stable compared to the PdO(100) plane [18]. This would indicate that the (101) plane should appear more often than observed. In this study, the diffraction peaks corresponding to the PdO(100) plane were more frequent and with higher intensity than those for the PdO(101) plane. The stronger peaks for PdO(100) suggest a more well-formed oxide surface under the experimental conditions used. This does not support the theory that lower-energy surfaces are more likely to form and persist under varied oxidative conditions [19]. However one explanation to why the (100) plane is more prevalent then the (101) in this study and not aligning with previous research may be due to the (201) plane. The reason this plane forms may be caused by not reaching a high enough vacuum in the chamber however more research on this would be necessary to reach a strong conclusion. This plane has not been observed in previously mentioned studies and may thus affect the formation of the (101) plane more than that of the (100) plane. This is also likely connected to the hypotheses that initial oxide growth has a strong impact on subsequent oxide growth. [19]

Oxide formation of the (100) and (101) planes has previously been observed frequently.[20] This is also what was expected in this study where the (101) plane is believed to be more catalyctivly active. However the (201) was unexpectedly detected. The (201) plane was also the most reoccurring in this research. A possible way to find an explanation to why the (201) plane appears so frequently since it was unexpected, is to look at the atomic distances of the PdO(201) plane and Pd(100) surface.

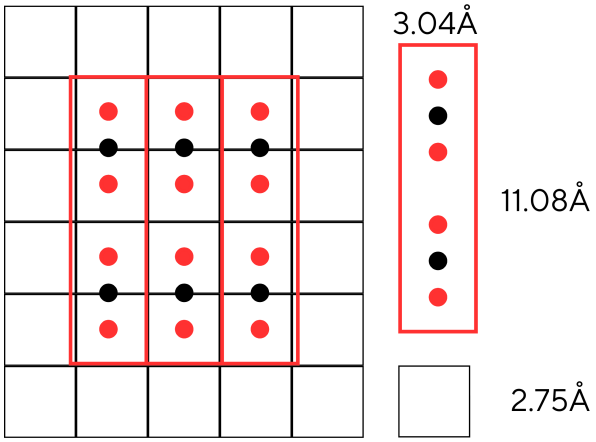

Figure 8: Crystal structure of Pd(100) surface in black and PdO(201) in red. All sides of the Pd unit cell has lengths 2.75 Å. The sides of PdO(201) has lengths 3.04 Å and 11.08 Å. There are atoms on each dot as well as on all corners.

From figure 8 we can see that the atomic distances between the Pd(100) bulk and the PdO(201) plane align quite closely. This lattice matching is crucial for epitaxial growth. Lattice mismatch can also induce strain at the interface which can lead to dislocations or other defects. This close alignment between Pd(100) and PdO(201) may

explain why the (201) plane forms under multiple different measurements and conditions.

Under the high-temperature conditions at 400°C, particularly at an oxygen pressure of 100 mbar O_2, a distinct behavior was observed in the PdO diffraction patterns. At two specific angles, which coincided with the bulk diffraction peaks of Pd, the PdO reflections appeared dispersed, forming almost a circular pattern. This dispersion suggests a highly disordered surface orientation of the PdO. However, the fact that this disorder only manifests at angles coinciding with the bulk diffraction peaks of the underlying Pd suggests that there is a preferential angle for the oxide formation. Despite this indication of a preferential angle, no preferred orientation of the oxide could be clearly distinguished.

This observation implies that while the oxide formation is influenced by the crystallographic orientation of the bulk Pd, the high temperature and oxygen pressure lead to a randomization of the PdO crystal orientation. This randomization could potentially be due to the dynamic conditions under which the oxides form, where the increased kinetic energy at higher temperatures allows atoms more freedom to occupy less energetically favorable positions, leading to a more disordered state.[18] Yet, the alignment with the bulk peaks suggests that the underlying crystal structure still exerts some influence over the process, possibly guiding the initial sites of oxide formation despite the subsequent disordering.

7 Conclusion

This study's investigation into the orientations of PdO growth on Pd(100) under varying environmental conditions has shed a light on the stability and formation of different PdO planes such as PdO(100), PdO(101), and PdO(201). Notably, the results confirmed that higher temperatures and increased oxygen pressures facilitate the formation of these planes and highlight the unexpected stability and recurrence of the PdO(201) plane, which had not been observed before.

Findings both in this study as well as previous studies show that the PdO(100) appears to be very stable and gives very strong peaks under various environmental circumstances. The relatively stronger diffraction peaks observed for PdO(100) compared to PdO(101) underlines this point along with the (201) orientation potentially disrupting the (101) orientation more than the (100) orientation suggest a potential preference in the (100) formation. The compatibility of the different planes in regards to the potency as a methane catalyst remains intriguing and now also comparing the (201) plane opens up further research directions. Although this specific aspect was not directly explored in the current study it would be interesting for future research.

The findings raise intriguing questions about the catalytic roles of different PdO planes, especially since the catalytic activity in methane oxidation of these surfaces was not directly measured. It remains speculative but highly probable that the different structural configurations of these planes might influence their effectiveness in catalytic applications. Why and when the different orientations form is an important step before more targeted approaches can be made potentially enhancing the efficiency of the catalytic process.

Future research should investigate the properties and potentials of the different PdO surfaces. Testing the catalytic activity of the various PdO planes directly, including the previously less common PdO(201), to show their effectiveness in methane oxidation. Additionally, employing theoretical and computational models to predict and verify the stability and catalytic activity of PdO surfaces based on their atomic configurations and environmental conditions. This provide insights that are not touched in this study and refine their applications in catalysis.

Additionally investigating whether the disorder on the surface is influenced by the order of operations, specifically, whether heating the sample after introducing O_2 differs from pre-heating the sample. Since oxides form more rapidly at higher pressures, the initial formation conditions significantly affect the subsequent surface structure. Once oxides form, they are challenging to "unform," suggesting that if the oxidation occurred solely at 400°C, the surface characteristics might be markedly different to the results observed in this study. This speculation is also strengthened by the fact that the formed oxides on the first and second set of measurements done at 350°C show different results. At 350°C the second measurement with pre-oxidation resulted in only the (100) orientation forming while the first measurement at 350°C resulted in the (100) orientation as well

as some additional (101) orientations. This could very well mean that the formation of the first oxides has a large impact on the oxide growth following after. This also reiterates the question whether heating the sample before introducing oxygen may have significantly differing results.

References

[1] A. Authier, “Early Days of X-ray Crystallography,” *Oxford University Press*, 2013.

[2] B.D. Cullity and S.R. Stock, “Elements of X-ray Diffraction,” 3rd ed., *Prentice Hall*, 2001.

[3] B.E. Warren, “X-ray Diffraction,” Dover Publications, 1990.

[4] F.C. Chung, “X-ray Diffraction for Materials Research: From Fundamentals to Applications,” Apple Academic Press, 2016.

[5] R.F. Giese Jr., “Introduction to Crystallography,” Dover Publications, 2019.

[6] W. Massa, “Crystal Structure Determination,” 2nd ed., Springer, 2012.

[7] A.M. Glazer and P.A. Maksimovich, “Fundamentals of Crystals: Symmetry, and Methods of Structural Crystallography,” Springer, 2019.

[8] R.L. Owen, et al., “Developments in X-ray detectors for synchrotron radiation,” *Journal of Synchrotron Radiation*, vol. 26, pp. 22-32, 2019.

[9] G.F. Knoll, “Radiation Detection and Measurement,” 4th ed., Wiley, 2010.

[10] M. Fiederle, “X-ray Detectors in Medical Imaging,” *Nuclear Instruments and Methods in Physics Research Section A*, vol. 731, pp. 112-117, 2013.

[11] M. Grant and J. H. Spurgeon, “Oxidation Theories in Material Science,” *Journal of Applied Physics*, vol. 115, pp. 1433-1446, 2018.

[12] C. T. Campbell, “The Surface Science of Metal Oxides,” *Surface Science Reports*, vol. 65, pp. 55-107, 2020.

[13] A. R. Overbury, “Thermodynamics and Kinetics of Oxidation for Metallic Surfaces,” *Progress in Surface Science*, vol. 94, pp. 112-134, 2019.

[14] I. V. Lazarev, “Phase Transformations of Elements Under High Pressure,” *CRC Press*, 2021.

[15] MDPI, “Pressure-Induced Phase Transformations (Volume II),” *MDPI*, 2020.

[16] J.G. McCarty, "Kinetics of PdO combustion catalysis," *Catalysis Today*, vol. 26, pp. 283-293, 1995.

[17] "Gibbs free energy of formation and heat capacity of PdO," *ScienceDirect*, 2021.

[18] J. Doe et al., "Comparative stability of PdO surfaces under oxidative environments," *Journal of Material Science*, vol. 58, pp. 1234-1245, 2023.

[19] M. Smith, "Thermodynamic and kinetic aspects of oxide surface stability," *Surface Science Reports*, vol. 78, pp. 456-489, 2022.

[20] A. Hellman, A. Resta, N. M. Martin, J. Gustafson, A. Trinchero, P.-A. Carlsson, O. Balmes, R. Felici, R. van Rijn, J. W. M. Frenken, J. N. Andersen, E. Lundgren, H. Grönbeck, "The Active Phase of Palladium during Methane Oxidation," *Journal of Physical Chemistry Letters*, 2012.